Journal of Rehabilitation in Civil Engineering 7-4 (2019) 01-17

Journal homepage: http://civiljournal.semnan.ac.ir/

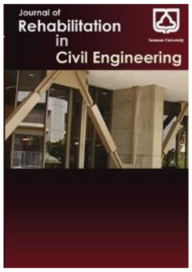

Experimental Strengthening of the Two-way Reinforced Concrete Slabs with High Performance Fiber Reinforced Cement Composites (HPFRCC) Prefabricated Sheets

M.M. Fallah[1], M. K. Sharbatdar[2*] and A. Kheyroddin[3]

1. Ph.D. Candidate, Faculty of Civil Engineering, Semnan University, Semnan, Iran
2. Associate Professor, Faculty of Civil Engineering, Semnan University, Semnan, Iran
3. Professor, Faculty of Civil Engineering, Semnan University, Semnan, Iran

Corresponding author: *msharbatdar@semnan.ac.ir*

ARTICLE INFO

Article history:
Received: 19 April 2018
Accepted: 14 July 2018

Keywords:
Two-Way Slab,
Poly Propylene Synthetic,
Fibers (*PPS)*Fibers,
Reinforcement,
HPFRCC,
Bending Performance,
Strengthening.

ABSTRACT

Reinforced concrete structures are required to be strengthened and retrofitted for various reasons, including errors during design and/or construction, so in most cases, strengthening of structural elements is much more economical than rebuilding the structure. Employing HPFRCC with tensile stiffening behavior has been developed in order to strengthen the concrete structures over the recent few years. In this paper, applying HPFRCC for strengthening two-way reinforced concrete slabs has been investigated. A total of five two-way slabs were constructed and examined to reach their own collapse stage, one of the specimen was as non-strengthened control slab, and the others were strengthened in various forms. The strengthening was carried out in two ways; by installing precast plate in the tensile area and the other by installing precast plate in both tensile and compression area at two different percentages of the fiber. The bending behavior, cracking, yielding and rupture of the experimental specimens were evaluated. The results revealed that the installation of HPFRCC pre-fabricated laminates significantly ameliorated the bending performance of reinforced slabs, so that the ductility, energy absorption value, cracking strength, and initial hardness of the slabs was increased and the crack width was decreased. Therefore, the proposed precast HPFRCC sheets can be employed in order to strengthen the deficient slabs.

1. Introduction

For various reasons such as designing and/or construction errors, a material deterioration in aggressive environment condition, damage as a result of earthquakes, converting the application of structure as well as the loss of

DOI: 10.22075/JRCE.2018.14532.1266

part of structural strength due to the corrosion of steel bars, many RC structures needs to be strengthened and retrofitted. Then again, strengthening the structural members is a lot more economical rather than reconstructing the structure in most cases. For this purpose, strengthening the RC structures has been much progressed during recent years. However, few researches have been conducted on RC slabs, especially on the strengthening of two-way slabs [1]. Strengthening the reinforced concrete slabs has been demonstrated by the various ways such as external post-tensioning, cross-sectional extending, reinforced cement cover, techniques of shortening the span, and adding the complementary supports [1]. In addition to the traditional strengthening methods, the performance of steel plates as external bond [2,3], strengthening with textile reinforced mortars (TRM)[4, 5], polyurethane cement composites (PUCs)[6], steel laminates, fibers reinforced polymer (FRP)[7,8], and the bonding techniques of these methods attracted many researchers' attention. These methods have been applied considerably; however , disadvantages such as undesirable shear failure, corrosion of bonded steel plates [9,10] and heavy laminates, mismatch in tensile strength and stiffness of FRP sheets and costly FRP sheets have led many researchers to perform many studies applying powerful materials with mechanical and behavioral properties similar to concrete as an alternative for the conventional materials, one of which is (HPFRCC). Namman and Reinhardt (2003) introduced the materials as HPFRCC that had tensile strain hardening in the strain-stress curve. HPFRCC materials have been classified separately from fiber-reinforced concrete (FRC), so that HPFRCC is a particular type of composites which their notable sing is the strain hardening behavior in post-crack tension that is accompanied with multiple cracks until they reach relatively large strains [11]. The studies by Chanvillard and Rigaud (2003) concluded a tensile strength of 12 MPa and tensile ductility of 0.02% - 0.06% [12]. Li (1993) and Fisher (2003)'s examination revealed a tensile strength of 4 to 6 MPa and tensile ductility of 3 to 5 % [13,14]. In 2006, the Technical Committee of RILEM decided to emphasize the strain hardening properties of these materials, so the name of Strain Hardening Cementitious Composites (SHCC) was selected for it [15]. Moreover, CARDIFRC materials, developed at Cardiff University, Wales, are one of a variety of HPFRCCs innovated by Farhat, Nicolaides, Kanellopoulos, and Karihalloo in 2006, and compressive strength was observed up to 200 MPa and a tensile strength up to 27 MPa [16] that main application of these materials is for repairing and amending the structural members. Habel And Gauvreau (2008) compounded concepts of ultra high performance concrete (UHPC) and fiber concrete and designed new materials named as ultra-high performance fiber reinforced concrete (UHPFRC) that tensile strength, compressive strength and ultimate tensile strain are higher than 10 MPa, 150 MPa and 0.005 respectively [17]. In 2009, Yoo et al. carried out some researches on improvement of the beam to concrete column connection behavior. The beam-to-column connection was strengthened with prefabricated fiber composite laminate. The results indicated that the initial hardness of the strengthened sample was reduced, yet its resistance was reported to be increased by 15%. The amount of energy depletion was another factor that increased as well [18]. In 2015, Hemmati et al. performed experimental and parametric studies to evaluate the effect of compressive strength, loading type and tensile reinforcement ratio on the characteristics of the final deformation of the reinforced HPFRCC beams and displayed that if the loading conditions are alternated from concentrated to monotonic loading, the plastic hinge rotation capacity is increased [19, 20, 21]. In 2015, Behzard et al. carried out an investigation for the effectiveness of a novel Near Surface Mounted (NSM) technique using innovative manually Made CFRP Rods (MMRs) and manually made CFRP strips (MMSs) for flexural strengthening of Reinforced Concrete (RC) two-way slabs with low clear cover thickness. The test results confirmed the feasibility and efficacy of this technique in improving the behavior of the RC two- way slabs. Strengthened slabs displayed a boost in flexural capacity between 279% and 394% over the control specimen [22]. In 2016, Khairaldin et al. have conducted some researches on increasing the capacity of the reinforced concrete frame using HPFRCC materials in a numerical way. In these models, the connecting span was replaced by HPFRCC materials with different tensile and compressive strengths then was compared with complete concrete frames and complete HPFRCC. The results indicated that the use of these high-performance materials can increase the load-bearing capacity and ductility of these frames [23]. In 2017, Abasszade et al. arranged an experimental program to inspect the effectiveness of employing two innovative methods near-surface mounted (NSM) techniques and HPFRCC Composites for improvement RC middle two-way slabs. The results confirmed the Strengthened slabs revealed a boost in flexural capacity between 17.5% and 97% over the control specimen [24].

In recent years, studies on the application of HPFRCC materials have been focused mostly on the cases such as the effects of bonding conditions between the substrate concrete and the laminate of HPFRCC [25], the layer thickness [26], the fiber volume percentage and the properties of the HPFRCC mix [27], crack growth and propagation [28], optimization and optimization and flexural performance [29, 30] and tensile strain-hardening behavior [31]. Recently, the feasibility of employing HPFRCC for the strengthening of the deficient or damaged slab and beam has been inquired widely [26, 32, 33]. In this paper, the feasibility of applying HPFRCC composites has been inquired as a slab, and various applications and settings for HPFRCC have been proposed. Subsequently, the load-displacement curves obtained from the tested slabs and some of the parameters of the flexural performance of them, such as energy absorption capacity, ductility factors, initial stiffness and maximum resistance, were evaluated.

2. Experimental Plan

2.1 Materials Properties

The used gravel in the applied concrete had a fracture percentage of 47% located in the sieve range of 0.5 inches (12.5 mm) to the 4 (4.75 mm). The sand utilized in this test is also in the blow sieve range of 4 (4.75 mm). The sand and gravel grading curves are portrayed in Fig. 1. The cement used in this test is Portland type 2 cement.

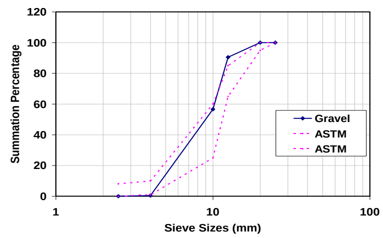

A- Gravel

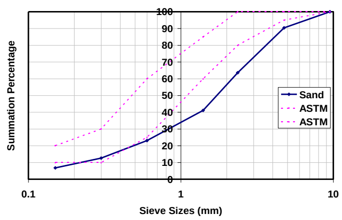

B- Sand

Fig. 1. Grading curves of sand and gravel.

Mixture design of conventional concrete utilized to cast reference and weak slabs are required to be strengthened as well as the mixture of HPFRCC as prefabricated strengthening sheets is illustrated in Table 1. The applied sand and gravel were dry. Therefore the extra water was considered. HPFRCC thin composites prefabricated sheets were installed with special two-part glue for flexural strengthening of the weak slabs. Since composite concrete with various fibers can apply in different forms for the slabs [25], Polypropylene synthetic *(PPS)* fibers with 1 and 2% volume percentage were employed for HPFRCC composite fabrication. This fiber has a length to diameter ratio (L/D) equal to 47.62 (length 50 mm and diameter of 1.05 mm), which is depicted in Fig. 2. The fibers were gradually added during the mixing process in order to prevent balling phenomena. The distribution of fibers in HPFRCC mix is presented in Fig. 2.

Plastiment sica super lubricant has also been applied in the ratio of HPFRCC mix.

(a) PPS fiber

(b) Ready Mortar

Fig. 2. PPS fibers and its distribution in HPFRCC mix.

Table 1. Ratio of conventional concrete and HPFRCC mortar mix (cubic meter).

Martial	Cement (kg)	Gravel (kg)		Sand (kg)	Water (kg)	Silica fume (kg)	Silica powder (kg)	Super plasticizer	PPS fiber (kg)
		2.36 < D < 4.75 (mm)	D< 2.36(mm)						
Concrete	405	662		1222	211	-	-	-	-
HPFRCC	846	422	716	-	254	84.60	25.40	8.50	8.46

In order to determine the compressive strength of two types of conventional and composite concrete, five cubic 10 × 10 cm were employed. The average compressive strength of the cube samples of the conventional concrete and HPFRCC concrete were equal to 23.5 and 74.5 MPa, respectively and the equivalent value of cylindrical samples of these two types of concrete were approximately 19 and 59 MPa. Steel bars with a diameter of 10 mm were selected from the type of thread class of AII, which the yielding strength of the rebar obtained using uni-axial tension tests was equal to 366 MPa.

2.2 Experimental Specimens and Set-Up

Five simply-supported rectangular two-way RC slabs with a geometric dimension length of 1500mm, width 1500mm and depth 100mm were constructed and tested. Two-way slabs with a low ratio longitudinal bar were designed in order to carry out flexural dominate failure and preventing any possible punch shear failure, the two-way slabs with a reinforcement ratio of 1% and higher are prone to shear failure caused by punching [3٤] ,thus to ensure prediction of flexural failure mode in the slabs and to inquire the effects of the strengthening technique, the slabs were designed with a low reinforcement ratio about the minimum reinforcement ratio (0.2%) according to the regulation of ACI 318-99 [33]. Therefore, 5 steel rebars with a diameter of 10 mm, at a distance of 130 mm on each side, with an average effective depth of 75 mm, have been set up in a layer near the slab tensile face. The anchorage of bars was provided by 180-degree hooks at both ends. The general layout of test samples and steel reinforcement details are exhibited in Figure 3.

The specimen details are indicated in Table 2. One of these five specimens was as a non-strengthened weak reference (control slab) named M and four other similar specimens were strengthened with different techniques. Two specimens of the second (MB1) and fourth (MA1) were strengthened with HPFRCC composites sheets contained 1% fibers and two specimens of the third (MB2) and fifth (MA2) specimen were fabricated with HPFRCC composites contained 2% fiber. In the second and third specimens, the composite cover was installed only on the lower tensile face of slab and in the fourth and fifth specimens simultaneously, the composite sheets was installed on the tensile and compressive face of the slab, more complete details are revealed in Figure 4. HPFRCC composites were individually fabricated in a mold with dimensions of 1000 x 1000 x 30 mm and, after reaching the age of 28 days, they were installed to the slabs faces with special two-component adhesives. To ensure that the connection is properly made, firstly, the slab surfaces are grinded and completely smoothed.

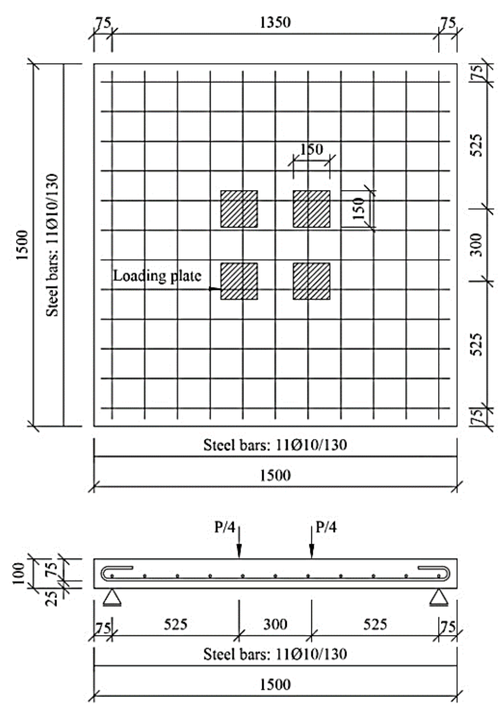

Fig. 3. General layout of a test specimen and details of steel reinforcements.

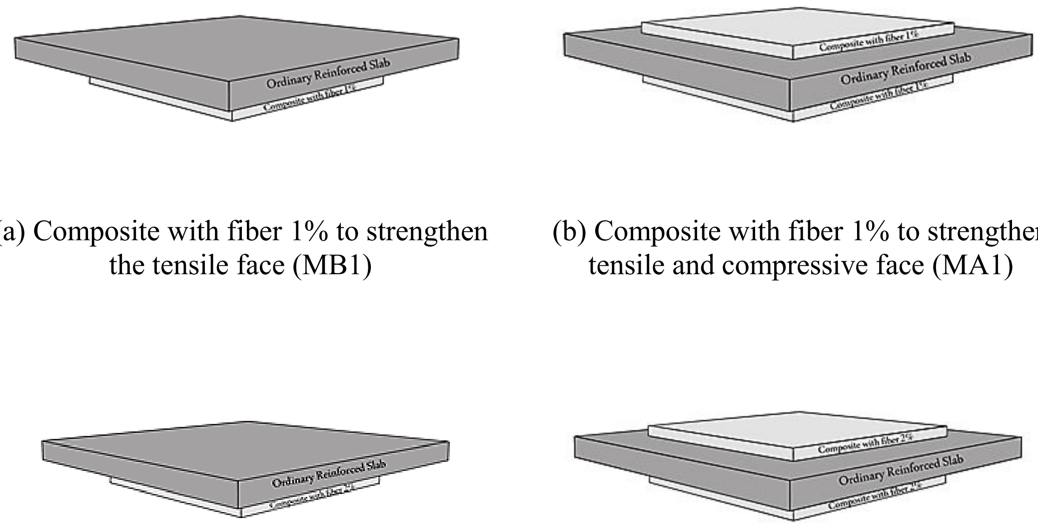

(a) Composite with fiber 1% to strengthen the tensile face (MB1)

(b) Composite with fiber 1% to strengthen tensile and compressive face (MA1)

(c) Composite with fiber 2% for strengthening tensile face (MB2)

(d) composite with 2% fiber to strengthen tensile and compressive face (MA2)

Fig. 4. Layout of strengthened forms.

Table 2. The Details tested specimens and strengthening methods.

Specimen No.	Name of slab	Type of concrete slab	Upper layer	Lower layer	Fibre volume percentage (%)	
		Mean	composite laminate HPFRCC	composite laminate HPFRCC	1	2
1	M	✓	–	–	–	–
2	MB1	✓	–	✓	✓	-
3	MB2	✓	–	✓	-	✓
4	MA1	✓	✓	✓	✓	-
5	MA2	✓	✓	✓	-	✓

First, the considered strengthened and non-strengthened slabs are placed on four 1,350 mm steel rollers embedded on top of the supporting frame as roller support in accordance with the edges. A 500 kN hydraulic jack was applied to examine the slab failure under monotonic loading. These loads were transmitted to the slab employing a distributor steel beam, through four loading points presented in Figure 5. The loading points and supports were selected to provide an effective 1,350 mm span and a 300 mm slit opening in both directions, as displayed in Figure 5. Vertical displacements of each tested specimen were measured at different positions in two directions perpendicular to each other using the linear variable displacement transducer (LVDT) mounted on a rigid metal base placed individually below the slab, displayed in Figure 6. One of the LVDTs is placed below the center of the slab and the four LVDTs were placed in the direction of the central lines of the slab to measure the raise at 300 and 550 mm from the center of the slab.

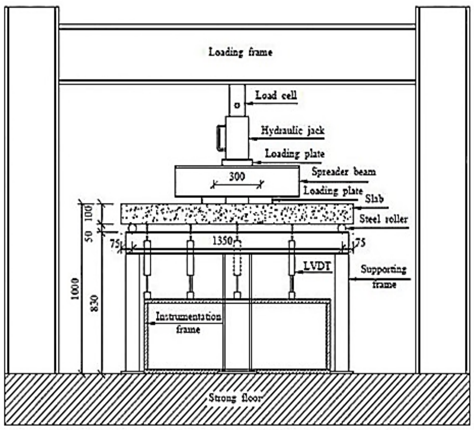

a) schematic

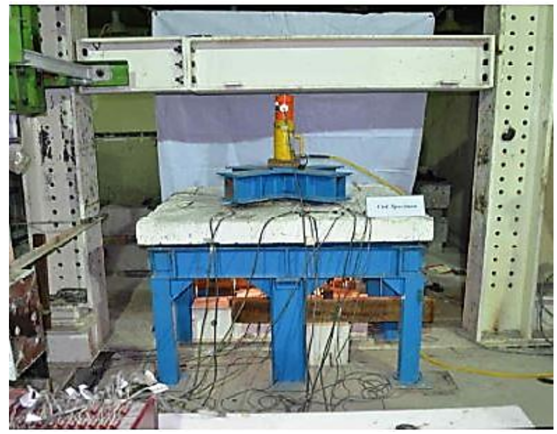

b) real

Fig. 5. Layout of the general test setup.

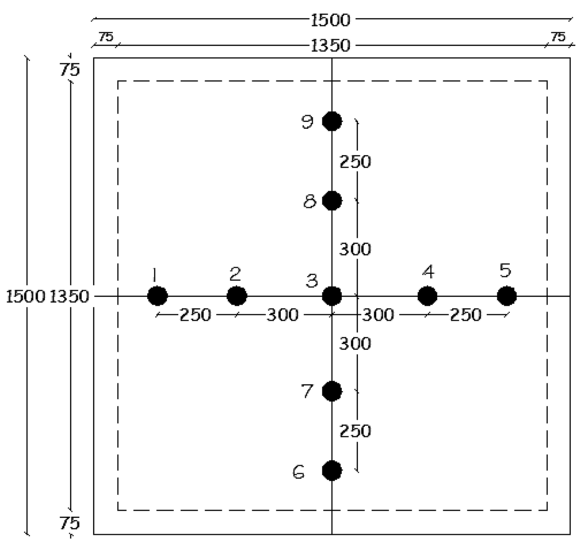

Fig. 6. Location of LVDTs.

3. Results and Discussion

The results acquired from the experiments are presented in the later sections as the load-displacement curves, the comparison of the failure modes, the cracking pattern, values of strength loads, displacement and energy ductility, the excessive resistance and the maximum resistance.

3.1. Load Displacement Response

The load-displacement response curves of the control weak reference specimen in comparison with the other four slabs which have been strengthened with HPFRCC composites are depicted in Figure 7. The maximum displacement recorded at the center of the slab in each loading stage is used to draw the load-displacement curve.

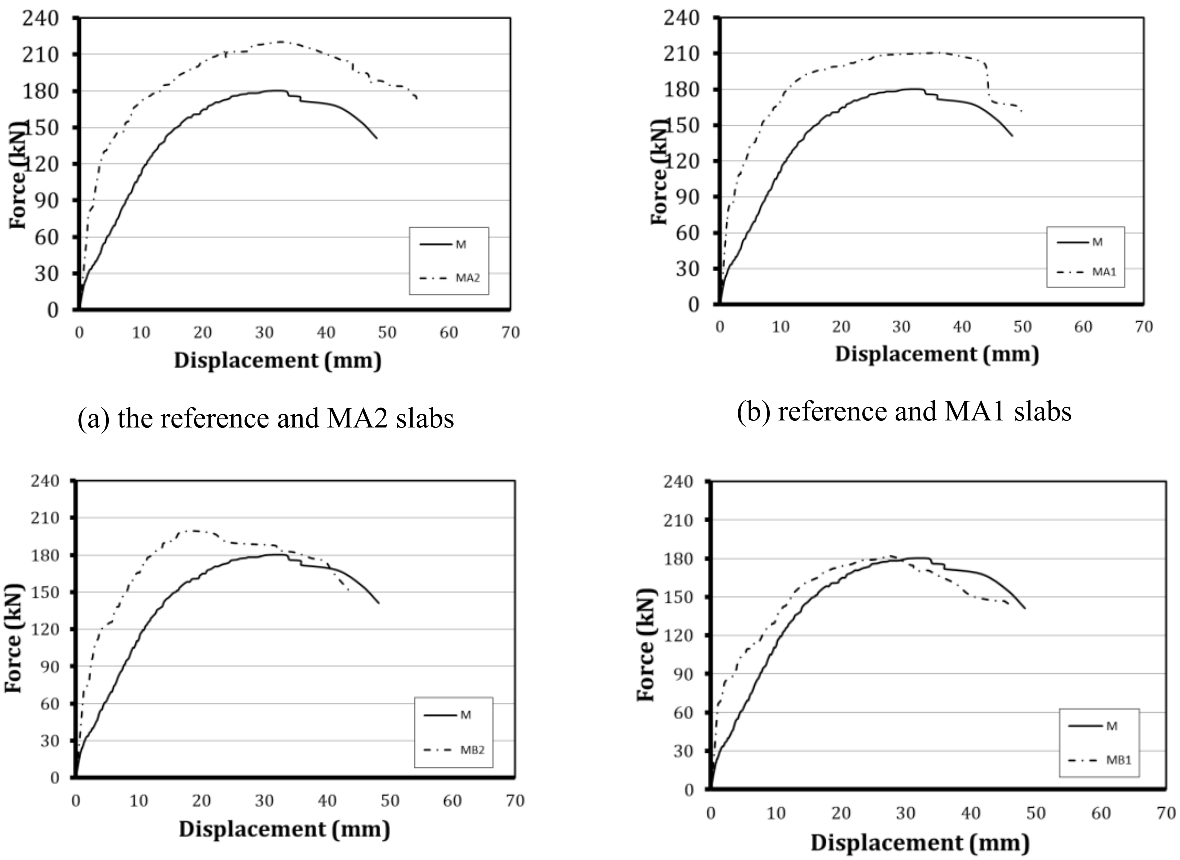

(a) the reference and MA2 slabs

(b) reference and MA1 slabs

(c) reference and MB2 slabs

(d) reference and MB1 slabs

Fig. 7. Load-displacement curves of weak reference slab in comparison with the strengthened slabs.

A summary of the results of this study, including the cracking, yielding and ultimate load and their corresponding displacements (the center) have been presented for all specimens in Tables 3 and 4. In the mentioned tables, Pcr **and** Δ_{cr} respectively, load and displacement corresponding to the cracking load, and P_y Δ_y determine the yielding load and the displacement corresponding to the yielding load, and $P_{\max}$ $\Delta_{\max}$ are the maximum load and raise corresponding to it, P_u **and** Δ_u ultimate loading capacity and displacement corresponding to the ultimate slab load. Indeed Δ_u indicates the slab load-displacement in 20% load drop after the maximum load. In P_y **&** Δ_y value, the proposed method of Park Robert has been employed, as depicted in Figure 8. In general, the load-displacement response is divided into two stages before cracking and the post-cracking stage. The cracked stage can be divided into two stages such as before yield and after yield stages. The cracked stage before yield is from cracking load (P_{cr}) to yield load (P_y). The cracked stage, after yield, continues from the yield (P_y) to the ultimate load (P_u).

Table 3. Load -displacement response parameters of slabs in cracking and yielding resistances.

Specimen	Cracking		Initial stiffness k_i(kN/mm)	$\frac{k_i}{k_{i-w}}$	Yield		$\frac{P_y}{P_{y-w}}$	Yield stiffness k_y (kN/mm)	$\frac{k_y}{k_{y-w}}$
	Δ_{cr} (mm)	P_{cr} (kN)			Δ_y (mm)	P_y (kN)			
Control(M)	0.8	21.60	27	1	17.50	157.7	1	9.01	1
MB1	1.14	67.17	58.92	2.18	14.35	160.5	1.02	11.18	1.23
MB2	1.33	73.16	55.01	2.04	9.5	165.56	1.05	17.43	1.92
MA1	1.72	85.83	49.90	1.85	10.90	178.6	1.13	16.38	1.80
MA2	1.88	80	42.55	1.58	12.65	179.2	1.14	14.17	1.56

Table 4. Load - displacement response parameters of slabs in maximum and ultimate resistances.

Specimen	Maximum		$\frac{P_{\max}}{P_{\max-M}}$	Maximum stiffness $k_{\max}$ (kN / mm)	$\frac{k_{\max}}{k_{\max-M}}$	Ultimate		Ultimate stiffness k_u (kN /mm)	$\frac{K_u}{K_{u-M}}$
	$\Delta_{\max}$ (mm)	$P_{\max}$ (kN)				Δ_u (mm)	P_u (kN)		
Control (M)	33.47	180	1	5.38	1	48.52	144	2.97	1
MB1	27.18	182.33	1.01	6.71	1.25	45.80	145.86	3.18	1.07
MB2	18.45	199.5	1.11	10.81	2.01	42.05	159.60	3.59	1.21
MA1	36.30	210.67	1.17	5.80	1.08	45.30	168.53	3.72	1.25
MA2	32.42	220.33	1.22	6.80	1.26	54.35	176.26	3.24	1.09

Since the visual observation of the first cracking in the under the face of the slab is not possible with sufficient precision, then the first cracking load can be considered as the point where the load-displacement response from the initial elastic response is diverted. The yielding load can be defined as the load that leads to strain in steel bars equal to the yield curve measured from the tension tests. Moreover, in the yield load, there is a significant alternation in the slope of the load-displacement curve. The ultimate load is the maximum tolerable load by the specimen (load-bearing capacity of the specimen). Deliberating the load-displacement response curves, it can be observed that the strengthened slabs had the initial hardness far more than the reference slab from the first stage. Further, in all samples, the yield strength and maximum, and finally, the ductility and energy absorption rate have been ameliorated significantly.

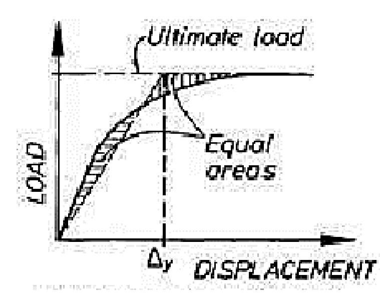

Fig. 8. determiner Curve of the yield resistance by Park Robert method [35].

3.2. Comparison of Failure Mode and Cracking Pattern

By comparing the failure patterns of the specimens in Figures 9 and 10, it was observed that the strengthened specimens showed a more ductility behavior than the control specimen. All strengthened specimens had a lower crack width than the control specimen, the reason for this was the effect of strengthening HPFRCC in preventing crack propagation. Moreover, by comparing the load-displacement response of the specimens in Figure 7 and the results presented in Table 3, it can be observed that resistance to cracking and initial stiffness of the specimens was increased by strengthening with HPFRCC. A boost in cracking load in the strengthened specimens compared with control slab is attributed to the role of strengthened with HPFRCC composites in limiting the growth of cracks.

Cracking patterns in the tensile face (lower) of the control specimen in the failure stage are illustrated in Figure 10. The first crack in the control slab, which is a simulator of a weak slab behavior in bending, occurred in the form of a shield (Y) (pre-cracking stage). After the first crack and the slope alternation of the load-displacement curve, which represents the initial stiffness of the slab, the pre-yield cracking stage is begun, which continues until the yield of the tensile reinforcements. After yielding of steel bars, the slab is entered the third part of the behavioral curve, which is strain hardening. In this area, with increasing the applied load, the length of the flexural cracks reaches the edges then it turns into shear cracks with a 45-degree angle at the sides. These cracks were expanded with increasing force and reach themselves to the pressure section of the slab. Further, by comparing the cracking patterns in this section and the load-displacement response in section 3.1, it can be observed that the behavior of the MB1 and MB2 slabs in the pre-cracking stage was quite similar to that of the control slab. As a result to the presence of composites, these slabs were flowed at higher yield load. However, the behaviour of the MA1 and MA2 slabs in the pre-cracking stage differed from the control slab and displayed a great stiffness at this stage.

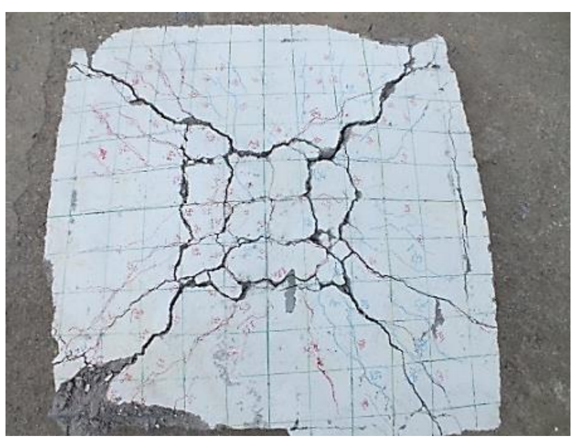

Fig. 9. The expansion of the flexural cracks and their movement toward the edge of the control slab.

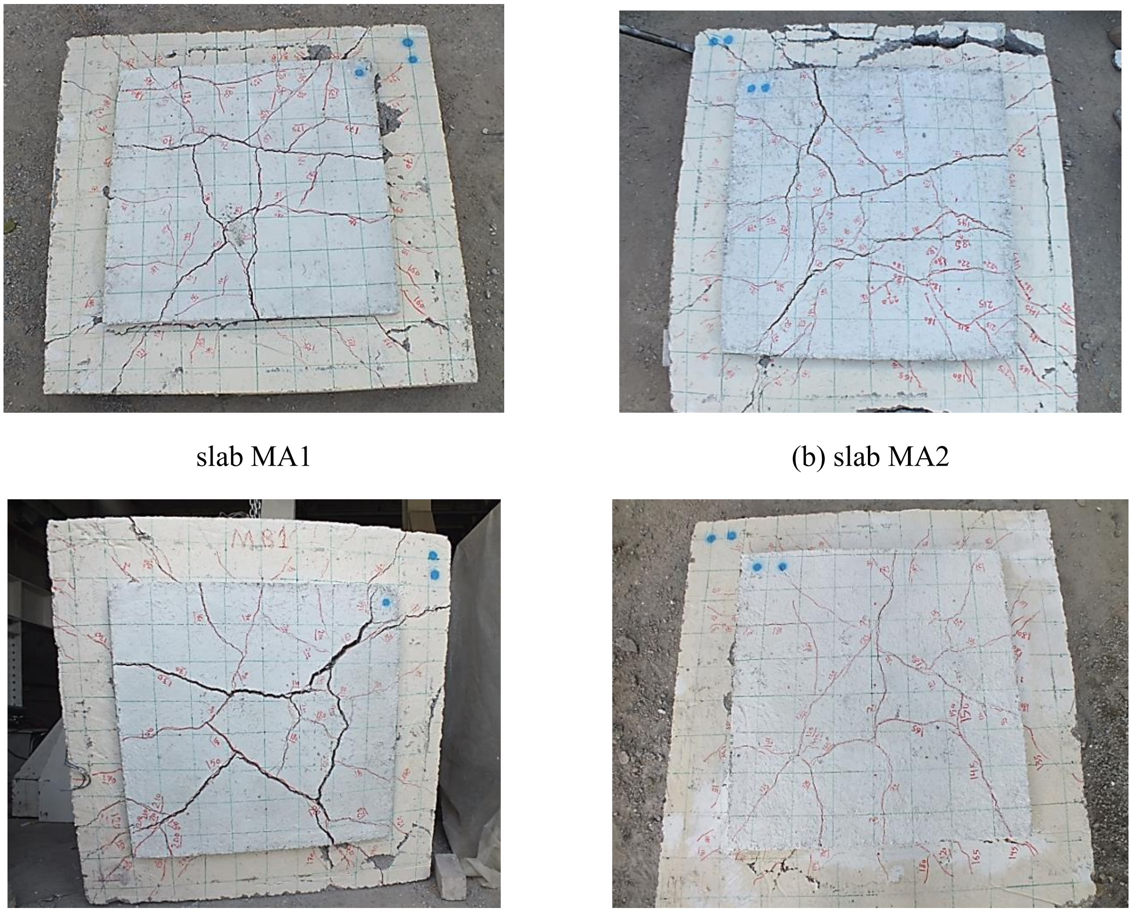

slab MA1 (b) slab MA2

(c) slab MB1 (d) slab MB2

Fig. 10. The expansion of the flexural cracks in the strengthened slabs.

3.3. Comparison of the Loads and Stiffness

The comparison of the cracking load (P_{cr}), yielding load (P_y), ultimate load (P_u) and their corresponding displacements (Δ_{cr}), (Δ_y) and (Δ_u) for all specimens are portrayed in Figures 11 and 12, respectively. Moreover, a comparison of the stiffness of the specimens at three cases of (k_{cr}), (k_y) and (k_u) are displayed in Figure 13. As expected, the initial stiffness (k_i), which was calculated through the load-displacement curve as the tangent stiffness of the un-cracked stage, all strengthened slabs had a higher value compared to the reference slab, and increase in the initial stiffness was as a result to increased cracking resistance and indicated the effect of HPFRCC composites. The strengthened slabs also received higher cracking values from the range of 67.17 kN in slab MB1 to 83.8 kN in slab MA1. A further increase in cracking load was observed in the strengthened slabs with a 1 and 2% fiber content was closed to each other and had a slight difference. This issue was also true for yield and maximum loads of the strengthened slabs, indicating that enhancing the fiber higher than 1% in slab load-bearing was not very effective, while the increase in load in two-way strengthened slabs is significant compared to one-way strengthened slabs. Pursuit to the diagrams in all samples, the amount of displacement was increased in cracking load and decreased in yield load. Decrease in the amount of displacement in the strengthened specimen was due to the hardening effects of the HPFRCC composites.

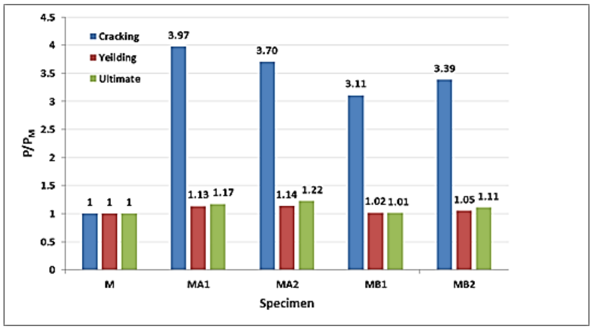

Fig. 11. Comparison of loads ratio in cracking, yielding, and ultimate modes.

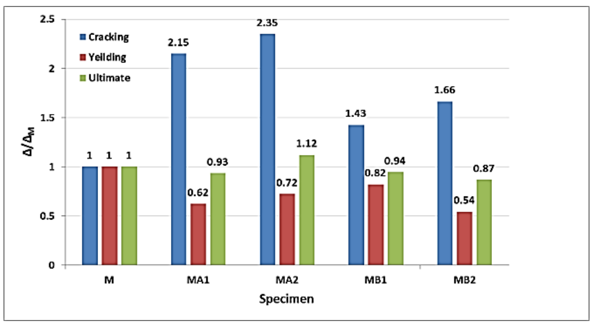

Fig. 12. Comparison of displacement ratio in cracking, yielding and ultimate modes.

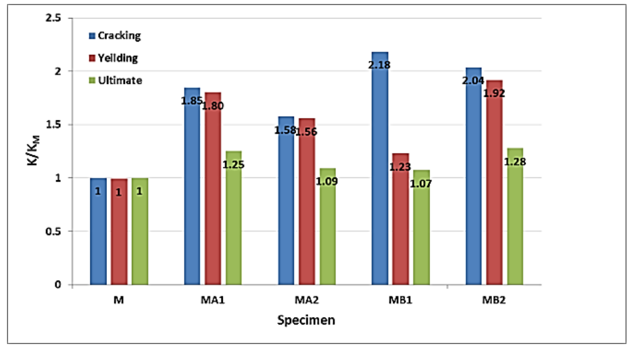

Fig. 13. Comparison of stiffness ratio in cracking, yielding and ultimate modes.

3.4. Energy Absorption

The energy absorption capacity of the slabs is evaluated by the area under the load-displacement curve. In order to compare the effect of different types of HPFRCC composites on increasing of weak slab strength, the tolerance values are computed in Table 5 and are drawn in Figure (14). As can be observed, energy absorption capacity has been increased in all slabs. Therefore, the energy absorption ratio was enhanced by 1 to 5 percent in slab strengthened only at the lower part, and 23 to 50 percent in the slabs strengthen at the top and bottom.

Table 5. Energy absorption capacity and ductility of the slabs.

Strengthen specimens	Energy absorption (kN.mm)	Energy absorption of each specimen to reference	$\mu_E = \frac{E_{u80\%}}{E_y}$	$\frac{\mu_{E(80\%)}}{\mu_{E(80\%)-W}}$	$\mu_\Delta = \frac{\Delta_{u80\%}}{\Delta_y}$	$\frac{\mu_\Delta}{\mu_{\Delta-w}}$	Excessive resistance factor $R=(P_{max}/P_y)$	$\frac{R}{R_w}$
Control(M)	6794.95	1	4.07	1	2.77	1	1.14	1
MB1	6859.26	1.01	4.25	1.04	3.74	1.35	1.22	1.07
MB2	7119.37	1.05	6.31	1.55	4.43	1.60	1.21	1.06
MA1	8327.61	1.23	6.11	1.50	4.16	1.50	1.18	1.03
MA2	10163.43	1.50	6.06	1.49	4.30	1.55	1.23	1.08

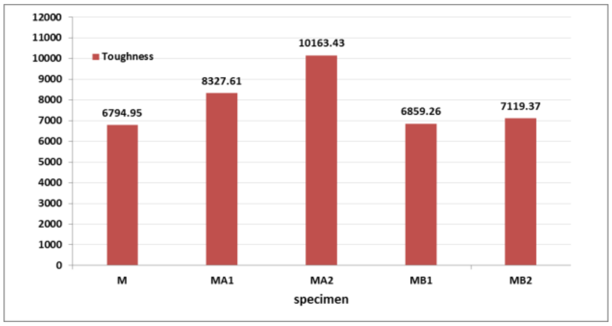

Fig. 14. Comparison of energy absorption of the samples.

3.5. Displacement and Energy of Specimens Ductility

Ductility is defined as the ability of the structure to tolerate the non-elastic displacements after the displacement of the first yielding in steel rebar without decreasing the bearing capacity of the structure and is introduced by a relation called the index or ductility coefficient (μ). Ductility index is usually defined as the ratio of displacement (Δ) or absorbed energy (E) at 20% load loss after the ultimate load of the specimen to the corresponding values at the yield load of the sample in consonance with equations 1, 2 and Figure 15.

$$\mu_{\Delta} = \frac{\Delta_{u80\%}}{\Delta_y} \qquad (1)$$

$$\mu_E = \frac{E_{u80\%}}{E_y} \qquad (2)$$

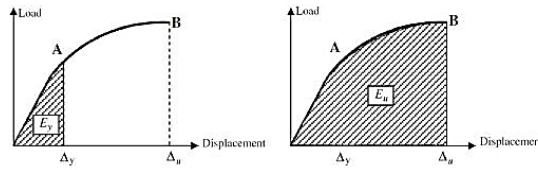

Fig. 15. Definition of the parameters for calculating the ductility of displacement and energy [33].

A comparison of the absorbed energy values and the displacement ductility of all five tested specimens is presented in Table 5. The column algorithm for comparing the displacement and energy ductility is displayed in Figures 16 and 17, respectively. As it is given, the displacement ductility of all samples was increased compared to the control sample, as well as the MB2 sample had the highest displacement ductility of 4.43. A similar trend was observed in the graphs for energy ductility.

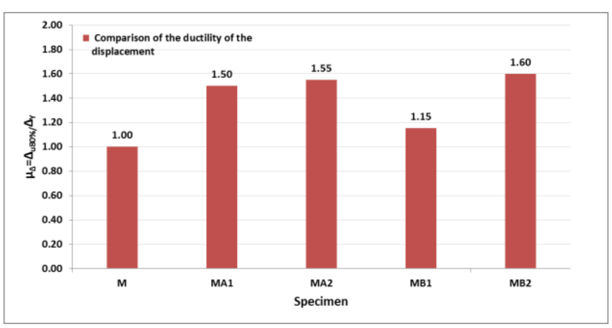

(a)

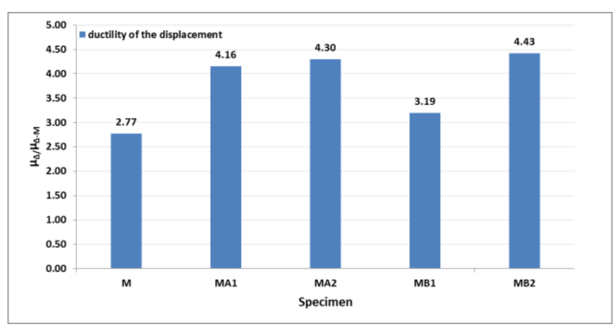

(b)

Fig. 16. Comparison of the displacement ductility of specimens.

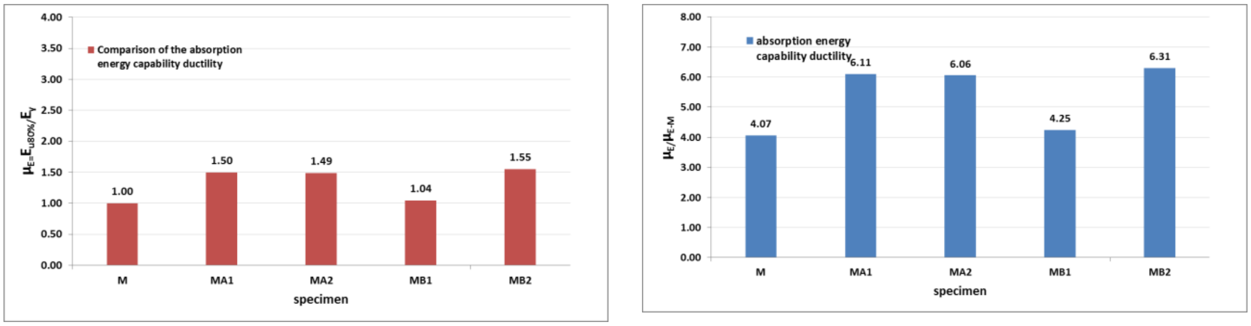

(a) **(b)**

Fig. 17. Comparison of the absorption energy ductility in specimens.

$$\text{Fig16:}\left\{a=\mu_{\Delta}=\frac{\Delta_{u80\%}}{\Delta_y}, b=\frac{\mu_{\Delta}}{\mu_{\Delta-M}}\right\}$$

$$\text{Fig17:}\left\{a=\mu_{E}=\frac{E_{u80\%}}{E_y}, b=\frac{E_{\Delta}}{E_{\Delta-M}}\right\}$$

By comparing the ductility values of the samples in this section and the load-displacement response in section 3.1, it can be observed that in samples with higher ductility, the load-bearing capacity decreased with a more moderate slope and was not accompanied with any sudden drop. Conversely, samples that had a lower degree of ductility exhibited a bitter behavior, and the load-bearing capacity was fell down suddenly in these samples.

3.6. Extensive Resistance Factor and Maximum Resistance

The coefficient of excessive resistance (R), which is influenced by factors such as the number of uncertain degrees of the structure, the strain hardening, the displacement constraints, the mechanical properties of the materials, and the strengthening pattern, is computed by an inelastic response curve, which is the ratio of maximum to yield loads of slabs specimens. The coefficient values of the excessive resistance are calculated for all samples and presented in Table 5. As presented in Figure 18, the maximum coefficient of excessive resistance of specimens has increased up to 23% in slab MA2.

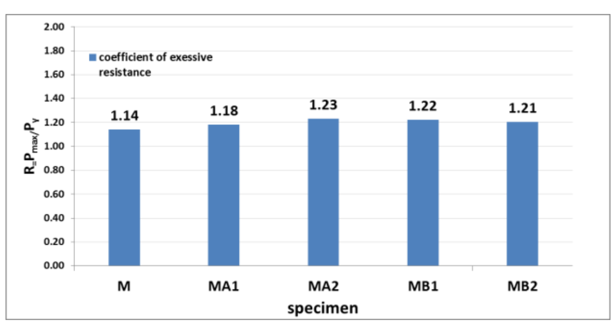

Fig. 18. Comparison of the coefficient values of samples resistance.

4. Conclusion

The results of experimental research on the application of HPFRCC composite pre-casted sheets for the strengthening of deficient slabs are presented as follow:

1. By comparing the specimen failure modes and the load-displacement response curves, it can be observed that the strengthened specimens exhibited a more ductility behavior than the control specimen.

2. All strengthened specimens have a lower crack width than the control specimen.

3. The cracking strength and initial stiffness of the specimens strengthened with HPFRCC were increased as a result to the limiting expansion of the cracks, so that the initial stiffness ratios in the specimens strengthened only at tensile face were 2.18 and 2.04 times of that of the control sample, and this ratio at specimens strengthened at both tensile and compressive faces were 1.58 and 1.85.

4. The yield and maximum load were increased respectively up to 14% and 22% in all strengthened specimens compared to the control sample. There was no significant difference between loads of specimens strengthened only at the tensile face at two cases of 1 and 2%. However, there was a difference at 1 and 2% fiber specimens strengthened at both tensile and compressive faces.

5. The energy absorption values of the slabs strengthened at both tensile and compressive faces were enhanced significantly up to 1.50 times of the energy value in the control slab.

6. The displacement ductility values in all strengthened specimens were increased by up to 60% compared to the control sample.

7. Excessive resistance coefficients in all slabs were increased up to 23% compare to control un-strengthened specimen.

REFERENCES

[1] Radomski, W. (2002). *Bridge rehabilitation*. London: Imperial College Press.

[2] Zhang, J. Teng, J. Wong, Y. and Lu, Z. (2001). Behavior of two-way RC slabs externally bonded with steel plate. *Journal of Structural Engineering*, 127(4), 390-397.

[3] Ebead, U. and Marzouk, H. (2002). Strengthening of two-way slabs using steel plates. *Structural Journal*. 99(1), 23-31.

[4] Papanicolaou, C. Triantafillou, T. Papantoniou, I. and Balioukos, C. (2009). Strengthening of two-way reinforced concrete slabs with textile reinforced mortars (TRM). In: *Proc of the 4th colloquium on textile reinforced structures (CTRS4) und zur 1. Anwendertagung*. Eigenverlag: Technische Universität Dresden, 409–420.

[5] Koutas, L. and Bournas, D. (2016). Flexural strengthening of two-way RC slabs with textile-reinforced mortar: experimental investigation and design equations. *Journal of Composites for Construction*. 21(1), 04016065.

[6] Kexin, Z. and Quansheng, S. (2016). Strengthening of a Reinforced Concrete Bridge with Polyurethane-cement Composite (PUC). *The Open Civil Engineering Journal*, 10(1), 768-781.

[7] Limam, O. Foret, G. and Ehrlacher, A. (2003). RC two-way slabs strengthened with CFRP strips: experimental study and a limit analysis approach. *Composite Structures*, 60(4), 467-471.

[8] Qian, K. and Li, B. (2012). Strengthening and retrofitting of RC flat slabs to mitigate progressive collapse by externally bonded CFRP laminates. *Journal of Composites for Construction*, 17(4), 554-565.

[9] Jones, R. Swamy, R. and Charif, A. (1988). Plate separation and anchorage of reinforced concrete beams strengthened by epoxy-bonded steel plates. *Structural Engineer*, 66(5).

[10] Hussain, M. Sharif, A. Bauch, I, Al Sulaimani, G. (1995) Flexural behavior of precracked reinforced concrete beams strengthened externally by steel plates. *Structural Journal*, 92(1), 14-23.

[11] Naaman, A. and Rienhardt, H.W. (2003). Setting the Stage, Toward Performance Based Classification of FRC Composites. In: *High Performance Fiber Reinforced Cement Composites (HPFRCC 4), Proc. of the 4th Int. RILEM Workshop, concrete journal*, 43(6), 57-62.

[12] Chanvillard, G. and Rigaud, S. (2003). Complete characterization of tensile properties of Ductal UHPFRC according to the French recommendations. In: *Proceedings of the 4th International RILEM workshop High Performance Fiber Reinforced Cementitious Composites*, RILEM Publications SARL, 21-34.

[13] Li, V.C. (1993). From micromechanics to structural engineering-the design of cementitous composites for civil engineering applications.

[14] FISCHER, G. and Shuxin, W. (2003). Design of engineered cementitious composites (ECC) for processing and workability requirements, in: Brittle Matrix Composites 7. Elsevier, 29-36.

[15] Rosenblueth, E. and Meli, R. (1986). The 1985 Mexico earthquake. *Concrete international*, 8(5), 23-34.

[16] Farhat, F. Nicolaides, D. Kanellopoulos, A. and Karihaloo, B. (2007). High performance fibre-reinforced cementitious composite (CARDIFRC)–Performance and application to retrofitting. *Engineering fracture mechanics*, 74(1-2), 151-167.

[17] Habel, K. and Gauvreau, P. (2008). Response of ultra-high performance fiber reinforced concrete (UHPFRC) to impact and static loading. *Cement and Concrete Composites*, 30(10), 938-946.

[18] Choi, W. Yun, H. Cho, Ch. And Feo, L. (2014). Attempts to apply high performance fiber-reinforced cement composite (HPFRCC) to infrastructures in South Korea. Composite Structures, 109, 211-223.

[19] Hemmati, A. Kheyroddin, A. and Sharbatdar, M.K. (2015). Increasing the flexural capacity of RC beams using partially HPFRCC layers. Computers and Concrete, 16(4), 545-568.

[20] Hemmati, A., Kheyroddin, A., Sharbatdar, M.K., "Flexural Behavior of Reinforced HPFRCC Beams", Journal of Rihabilitation in Civil Engieering, Vol. 1 (2013) 66-77.

[21] Hemmati, A., Kheyroddin, A. and Sharbatdar, M.K. (2014), "Plastic hinge rotation capacity of reinforced HPFRCC beams", J. Struct. Eng., 141(2), 04014111.

[22] Behzard, P. Sharbatdar, M.K. and Kheyroddin, A. (2016). A different NSM FRP technique for strengthening of RC two-way slabs with low clear cover thickness. Scientia Iranica A, 23(2), 520-534.

[23] Hemmati, A. Kheyroddin, A. Sharbatdar, M.K. Park, Y. and Abolmaali, A. (2016). Ductile behavior of high performance fiber reinforced cementitious composite (HPFRCC) frames. Construction and Building Materials, 115, 681-689.

[24] Abbaszade, M.A. Sharbatdar, M.K. and Kheyroddin, A. (2017). Strain Hardening Cementitous Comosites for Retrofitting Two-Way RC Slabs. Journal of Fundamental and Applied Sciences, 9(2), 1251-1282.

[25] Alaee, F. (2002). Retrofitting of concrete structures using high performance fibre reinforced cementitious composite (HPFRCC). Cardiff University.

[26] Yun, H.-D. Rokugo, K. Izuka, T. and Lim, S. (2011). Crack-damage mitigation of RC one-way slabs with a strain-hardening cement-based composite layer. *Magazine of Concrete Research*, 63(7), 493-509.

[27] Naghibdehi, M. Mastali, M. Sharbatdar, M.K. and Naghibdehi, M.G. (2014). Flexural performance of functionally graded RC cross-section with steel and PP fibres. *Magazine of Concrete Research*, 66(5), 219-233.

[28] Banthia, N. and Nandakumar, N. (2003). Crack growth resistance of hybrid fiber reinforced cement composites. *Cement and Concrete Composites*, 25(1), 1-9.

[29] Meng, W. and Khayat, K.H. (2017). Improving flexural performance of ultra-high-performance concrete by rheology control of suspending mortar. *Composites Part B: Engineering*, 117, 26-34.

[30] Meng, W. Valipour, M. and Khayat, K.H. (2017). Optimization and performance of cost-effective ultra-high performance concrete. *Materials and structures*, 50(1), 29.

[31] Li, V.C. Wang, S. Wang, Sh, and Wu, C. (2001). Tensile strain-hardening behavior of polyvinyl alcohol engineered cementitious composite (PVA-ECC). *ACI Materials Journal-American Concrete Institute*, 98(6), 483-492.

[32] Hemmati, A. Kheyroddin, A. and Sharbatdar, M.K. (2013). Plastic hinge rotation capacity of reinforced HPFRCC beams. *Journal of Structural Engineering*, 141(2), 04014111.

[33] Meng, W. and Khayat, K.H. (2016). Experimental and Numerical Studies on Flexural Behavior of Ultrahigh-Performance Concrete Panels Reinforced with Embedded Glass Fiber-Reinforced Polymer Grids. *Transportation Research Record: Journal of the Transportation Research Board*, 2592, 38-44.

[34] Afefy, H. and Fawzy, T.M. (2013). Strengthening of RC one-way slabs including cut-out using different techniques. *Engineering Structures*, 57, 23-36.

[35] Robert, Park. (1998). *Ductility evalution from laboratory and analytical testing. Tokyo-Kyoto, JAPAN:* Ninth world Conference on Earthquake Engineering, 606-607.